AIMS Mathematics, 7(9): 16673–16691.
DOI:10.3934/math.2022914
Received: 02 April 2022
Revised: 16 June 2022
Accepted: 23 June 2022
Published: 12 July 2022

http://www.aimspress.com/journal/Math

Research article

Dynamic optimal operational control for complex systems with nonlinear external loop disturbances

Liping Yin, Yangyu Zhu, Yangbo Xu and Tao Li*

CICAEET, Nanjing University of Information Science and Technology, No. 219, Ningliu Road, Nanjing, 210044, China

* **Correspondence:** Email: taolinanjing@163.com; Tel: 02558731059.

Abstract: This paper studies a two-layer control strategy for optimal operational control which is prevalent in industrial production. The upper layer determines and adjusts the target set values, while the lower layer makes the loop output track the target value. In the two-layer structure optimal setting control system, the widely used PID controller is used in the bottom layer. Firstly, the parameters of the PID controller are obtained by solving linear matrix inequalities (LMI). Secondly, for industrial processes with nonlinear harmonic disturbances, a disturbance observer is designed to estimate these disturbances. Thirdly, the effects of disturbances or noises are minimized by dynamically adjusting the setting points. This method does not change the structure or parameters of the bottom controller, and thus meets the actual industrial requirements to a certain extent. Finally, in the numerical simulation section, the value of the performance index before set-points adjustment is compared with that after set-points adjustment.

Keywords: optimal operational control; PID; nonlinear; disturbance observer; set-points reselection
Mathematics Subject Classification: 93C10, 93D05

1. Introduction

With the development of modern industry and the increasingly fierce competition in the world market, new requirements are continually put forward to the production control process by industrial departments, which not only require the output of controlled equipment to track its set value to the greatest extent, but also require good control of the operation of the whole industrial equipment to improve the production quality, efficiency and energy consumption within some range. In fact, the optimal operational control of many complex industrial processes consists of two layers-loop control layer and operation control layer [1], which is shown in Figure 1. In Figure 1, the goal of the loop control layer is to control the output of each loop on the production line, and the operation control

layer is to dynamically adjust the set value of each loop to optimize the performance index such that the value of the production performance index (such as economic profit or production cost) run with the target range [2–8].

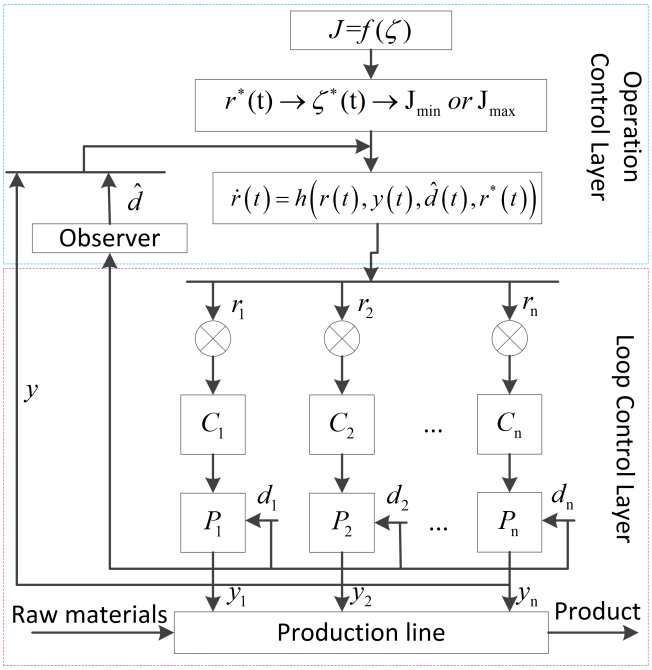

Figure 1. Schematic diagram of two-layered optimal setting control.

As we know, in some industrial production processes, once the production line is completed, the underlying controller structure is difficult to change, so it is unrealistic to redesign the bottom layer controller [9–14]. Moreover, the range of controller parameters adjustment is usually limited, and thus the optimal operation of the whole production line is not easy to be realized. At present, many literatures have studied other ways to improve the system performance on the premise of using fixed controller, for example, the fixed multi-loop PID control is adopted for the grinding process to reduce the particle size of ore and screen out valuable ore in [5] which shows that selecting appropriate set points also works to improve the whole performance. In [6], the fixed controller operation optimization method is applied for another industrial process called high concentration refining system in which the pulp quality target, economic target and energy consumption target were tracked respectively to set points. This method can significantly reduce the energy consumption for refining system and ensure ideal pulp quality. In order to make the optimization algorithm easier for goethite process, a fixed PID controller is also used in [14] to control the addition amount of zinc oxide and oxygen during operation, and an optimization method is adopted based on set point tracking strategy to convert complex state constraints into additional objectives, which can not only suppress disturbances, but also reduce raw material consumption in the production process.

On the other hand, many practical systems are influenced by input (output) constraints, multiple objective functions or noises [15–17]. When the basic site conditions change, the set point of each loop can be hardly found in real time if only based on the experience of engineers and operators, so the actual production can not always meet the technical requirements [18–20]. To this purpose, some

intelligent algorithms are adopted to optimize performance indices. For example, in [18], in order to improve the sewage purification efficiency, an adaptive multi-objective differential evolution algorithm is used to find the appropriate set point to balance the working performance and operating cost of the machine. In [19], a hybrid intelligent control optimization method is introduced based on multi-objective evaluation in the roasting process of the shaft furnace. The set value of each control loop is adjusted through real-time evaluation and on-line correction, which not only improves the combustion efficiency of the shaft furnace, but also reduces the equipment faults. In [20], a blade pitch parameter tuning optimization method is proposed based on intelligent genetic algorithm which rearranges the mutation rate and crossover points according to the algorithm progress, and more successfully adjusts the blade pitch of wind turbine under high wind speed.

Different from those intelligent optimization algorithms, this paper theoretically analyzes the relationship between the PID controller and upper layer set points, and studies an optimal operational control method with nonlinear harmonic disturbances. By designing a disturbance observer and dynamically resetting the set-points, the outputs of the nonlinear control loops can be tracked to the desired set points without changing the structure or parameters of the controllers.

The remainder of the paper is organized as follows: The optimal operational control process and the system model will be described in Section 2. The bottom layer controller will be designed in Section 3 and the disturbance observer will be designed in Section 4. In Section 5, the set points will be dynamically adjusted. The effectiveness of the method is verified by simulation in Section 6, and the conclusion is drawn in Section 7.

2. Problem description

Figure 1 is an industrial operation control process in which the operation indicators ξ^* can be obtained through the planning and scheduling of performance indicators J. During operation, engineers will determine the set point $r_j^*(j = 1, 2, \cdots, n)$ for each control loop according to experience, and the controllers will produce required inputs $u_j(t)(j = 1, 2, \cdots, n)$ to ensure that its outputs $y_j(t)(j = 1, 2, \cdots, n)$ track the set point r_j^* such that the overall performance can be optimized. In general industrial processes, the performance index J represents profit and energy cost, which can be usually written as:

$$J = \int_{T_0}^{T_f} [q_m(\tau)(p_u(\tau) - p_l(\tau)) - C_0(\tau)]d\tau, \tag{2.1}$$

where $q_m(\tau)$ is the product quantity in time interval $\left[T_0, T_f\right]$, $p_u(\tau)$ is the unit price function of the product at time τ, $p_l(\tau)$ is the unit price of raw materials, and $C_0(\tau)$ is the energy consumption.

In Figure 1, $d_i(t)$ is the disturbance in each loop. When there exist disturbances, the dynamic set point can be re selected and applied to the operation control layer as follows [2]:

$$\dot{r}(t) = h\left(r(t), y(t), \hat{d}(t), r^*(t)\right), \tag{2.2}$$

where $h(\cdot)$ is a unknown function with respect to the design of operation index $r^*(t)$, output $y(t)$ and disturbance estimation $\hat{d}(t)$, and $r(t)$ is the reselected set point.

In the two-layer system, it is assumed that the dynamic model of each bottom loop can be expressed as follows:

$$Loop_i : \begin{cases} \dot{x}_i(t) = A_i x_i(t) + B_i u_i(t) + f_i(x_i(t)) + d_i(t) \\ y_i(t) = C_i x_i(t) \end{cases} \quad i = 1, 2, \cdots, n, \tag{2.3}$$

where $x_i \in R^{n_i \times 1}$ is the state vector of each subsystem, $y_i \in R^{m_i \times 1}$ is the system output, $u_i \in R^{p_i \times 1}$ is the control input, $A_i \in R^{n_i \times n_i}$, $B_i \in R^{n_i \times p_i}$ and $C_i \in R^{m_i \times n_i}$ are the system matrices of the subsystem respectively, while $d_i \in R^{n_i \times 1}$ is the disturbance, and f_i is the nonlinear function which meets the following assumptions:

Assumption 2.1: For any $x_1(t)$ and $x_2(t)$, the nonlinear function $f_i(x(t))$ satisfies

$$\|f_i(x_1(t)) - f_i(x_2(t))\| \leq \|U_i(x_1(t) - x_2(t))\|, \tag{2.4}$$

where U_i are given Lipschitz constants and $\|\cdot\|$ stands for Euclidean norm for vectors.

The composite system for (2.3) can be written as:

$$\begin{cases} \dot{x}(t) = Ax(t) + Bu(t) + f(x(t)) + d(t), \\ y(t) = Cx(t), \end{cases} \tag{2.5}$$

where the composite vectors x, y, u are written as $x = \left[x_1^T, \cdots x_n^T\right]^T$, $y = \left[y_1^T, \cdots y_n^T\right]^T$, $u = \left[u_1^T, \cdots u_n^T\right]^T$; A, B and C are system matrices which are denoted as $A = diag\{A_1, \cdots, A_n\}$, $B = diag\{B_1, \cdots, B_n\}$ and $C = diag\{C_1, \cdots, C_n\}$, $d(t) = diag\{d_1, \cdots, d_n\}$.

Denote the tracking error as $\varepsilon(t)$, then it can be expressed as follows:

$$\varepsilon(t) = r^*(t) - y(t).$$

The residual $e(t)$ between the setpoint $r(t)$ and the actual control output $y(t)$ can be defined as

$$e(t) = r(t) - y(t).$$

If the disturbances are not considered, the relationship between the tracking error $\varepsilon(t)$ and residual $e(t)$ is as follows:

$$e(t) = \varepsilon(t) = r^*(t) - y(t).$$

3. Bottom layer controller design

Due to technical and economic constraints, PID controllers are still widely used in many industrial processes [21–29]. Because PID controllers are simple in structure and easy to operate, in order to make the algorithm in this paper more adaptive, this paper still uses PID control in the loop control layer shown in Figure 1, and tries to use LMI algorithms to determine the controller parameters. The PID controller of the loop control layer can be expressed as follows:

$$u(t) = K_P e(t) + K_I \int_0^t e(\tau) d\tau + K_D \dot{e}(t). \tag{3.1}$$

Substitute the PID control law (3.1) into (2.5), we get

$$\dot{x}(t) = Ax(t) + B\left(K_P e(t) + K_I \int_0^t e(\tau) d\tau + K_D \dot{e}(t)\right) + f(x(t)).$$

In the ideal case (without considering disturbance), $e(t) = \varepsilon(t) = r^*(t) - y(t)$, in order to make the algorithm more explicit, we assume that the state is measurable and let $C = I$, then

$$\begin{aligned}\dot{\varepsilon}(t) &= \dot{r}^*(t) - \dot{x}(t)\\ &= \dot{r}^*(t) - A(r^* - \varepsilon) - f(x(t)) - BK_P e(t) - BK_I \int_0^t e(\tau)d\tau - BK_D\dot{e}(t)\\ &= (A - BK_P)\varepsilon(t) - BK_I \int_0^t e(\tau)d\tau - BK_D\dot{e}(t) - f(x(t)) + \dot{r}^*(t) - Ar^*(t).\end{aligned} \tag{3.2}$$

Let $s(t) = \int_0^t \varepsilon(\tau)\, d\tau$, then

$$\begin{pmatrix} \dot{\varepsilon}(t) \\ \dot{s}(t) \end{pmatrix} = \begin{pmatrix} \Delta^{-1}\Pi & -\Delta^{-1}BK_I \\ I & 0 \end{pmatrix}\begin{pmatrix} \varepsilon(t) \\ s(t) \end{pmatrix} + \Delta^{-1}\begin{pmatrix} \dot{r}^*(t) - Ar^* \\ 0 \end{pmatrix} + \begin{pmatrix} \Delta^{-1}f(r^* - \varepsilon) \\ 0 \end{pmatrix}, \tag{3.3}$$

where $\Delta = I + BK_D$, $\Pi = A - BK_P$, and K_P, K_I, K_D represent the proportional coefficient, integral coefficient and differential coefficient of PID controller, respectively.

Theorem 3.1. If there exist $P > 0$, $K_P \in R^{m\times m}$, $K_I \in R^{m\times m}$ and $K_D \in R^{m\times m}$ such that the following two matrix inequalities hold

$$P = \begin{pmatrix} P_1 & P_2 \\ {P_2}^T & P_3 \end{pmatrix} > 0, \tag{3.4}$$

$$\begin{pmatrix} \Phi & \psi_1 & \psi_2 & \psi_3 \\ \psi_1^T & -I & 0 & 0 \\ \psi_2^T & 0 & -I & 0 \\ \psi_3^T & 0 & 0 & -I \end{pmatrix} < 0, \tag{3.5}$$

where

$$\Phi = \begin{pmatrix} \Phi_{11} & \Phi_{12} \\ \Phi_{12}^T & \Phi_{22} \end{pmatrix}, \tag{3.6}$$

$$\psi_1 = \lambda P\begin{pmatrix} \Delta^{-1} \\ 0 \end{pmatrix}, \psi_2 = \frac{\sqrt{2}}{\lambda}\begin{pmatrix} {U_1}^T \\ 0 \end{pmatrix}, \psi_3 = P\begin{pmatrix} \Delta^{-1}A \\ 0 \end{pmatrix},$$

$$\begin{aligned}\Phi_{11} &= sym\left(P_1\Delta^{-1}\Pi + P_2\right),\\ \Phi_{12} &= -P_1\Delta^{-1}BK_I + \Pi^T\Delta^{-T}P_2 + P_3,\\ \Phi_{22} &= sym\left(-P_2^T\Delta^{-1}BK_I\right),\end{aligned}$$

then the composite system (3.3) is asymptotically stable.

Proof. Construct the following Lyapunov function:

$$\begin{aligned}V_1 = &\begin{bmatrix} \varepsilon^T(t) & s^T(t) \end{bmatrix}\begin{bmatrix} P_1 & P_2 \\ P_2^T & P_3 \end{bmatrix}\begin{bmatrix} \varepsilon(t) \\ s(t) \end{bmatrix}\\ &+ \frac{1}{\lambda^2}\int_0^t \|U_1(r^* - \varepsilon(\tau))\|^2 - \|f(r^* - \varepsilon(\tau))\|^2 d\tau.\end{aligned} \tag{3.7}$$

Taking the derivative of $V_1(t)$ with respect to t yields

$$\begin{aligned}
\dot{V}_1 &= \begin{bmatrix} \varepsilon^T(t) & s^T(t) \end{bmatrix} \Phi \begin{bmatrix} \varepsilon(t) \\ s(t) \end{bmatrix} + 2 \begin{bmatrix} \varepsilon^T(t) & s^T(t) \end{bmatrix} P \begin{bmatrix} \Delta^{-1} \\ 0 \end{bmatrix} (\dot{r}^*(t) - Ar^*) \\
&\quad + 2 \begin{bmatrix} \varepsilon^T(t) & s^T(t) \end{bmatrix} P \begin{bmatrix} -\Delta^{-1} \\ 0 \end{bmatrix} f(r^* - \varepsilon(t)) + \frac{1}{\lambda^2} \left[\|U_1(r^* - \varepsilon(t))\|^2 - \|f(r^* - \varepsilon(t))\|^2 \right] \\
&\leq \begin{bmatrix} \varepsilon^T(t) & s^T(t) \end{bmatrix} \left[\Phi + \lambda P^2 \begin{bmatrix} \Delta^{-1}\Delta^{-T} & 0 \\ 0 & 0 \end{bmatrix} P^T + \begin{bmatrix} \frac{2}{\lambda^2} {U_1}^T U_1 & 0 \\ 0 & 0 \end{bmatrix} + P \begin{bmatrix} \Delta^{-1} A A^T \Delta^{-T} & 0 \\ 0 & 0 \end{bmatrix} P^T \right] \begin{bmatrix} \varepsilon(t) \\ s(t) \end{bmatrix} \\
&\quad + r^{*T} r^* + \frac{1}{\lambda^2} \dot{r}^{*T} U_1^T U_1 \dot{r}^* \\
&\leq -\sigma_0 \left\| \begin{pmatrix} \varepsilon \\ s \end{pmatrix} \right\|^2 + \lambda_{\max},
\end{aligned}$$

where $\lambda_{\max}$ is the maximum eigenvalue of matrix $r^{*T} r^* + \frac{1}{\lambda^2} \dot{r}^{*T} U_1^T U_1 \dot{r}^*$. Therefore, when $\left\| \begin{pmatrix} \varepsilon \\ s \end{pmatrix} \right\| \geq \sigma_0^{-\frac{1}{2}} {\lambda_{\max}}^{\frac{1}{2}}$, $\dot{V}_1 < 0$, and the state vector $\begin{pmatrix} \varepsilon^T & s^T \end{pmatrix}$ satisfies

$$\left\| \begin{pmatrix} \varepsilon(t) \\ s(t) \end{pmatrix} \right\| \leq \max \left\{ \sigma_0^{-\frac{1}{2}} {\lambda_{\max}}^{\frac{1}{2}}, \left\| \begin{pmatrix} \varepsilon(0) \\ s(0) \end{pmatrix} \right\| \right\}.$$

In the ideal case (without considering the disturbances), let $\theta(t)$ be the trajectory of the composite loop system (3.3), then

$$\lim_{t \to \infty} \theta(t) = \theta_0,$$

where θ_0 is a constant vector, and

$$\lim_{t \to \infty} \dot{\theta}(t) = 0,$$

because of $\dot{s}(t) = \varepsilon(t)$, we have

$$\lim_{t \to \infty} \varepsilon(t) = 0,$$

the proof is completed.

According to the Schur complement lemma [30], it can be easily proven that (3.5) in Theorem 3.1

$$\begin{bmatrix} \tilde{\Phi}_{11} & \tilde{\Phi}_{12} \\ \tilde{\Phi}_{12}^T & \tilde{\Phi}_{22} \end{bmatrix} < 0. \tag{3.8}$$

where

$$\begin{aligned}
\tilde{\Phi}_{11} &= \Phi_{11} + \lambda^2 P_1 \Delta^{-1} \Delta^{-T} P_1 + \tfrac{2}{\lambda^2} {U_1}^T U_1 + P_1 \Delta^{-1} A A^T \Delta^{-T} P_1, \\
\tilde{\Phi}_{12} &= \Phi_{12} + \lambda^2 P_1 \Delta^{-1} \Delta^{-T} P_2 + P_1 \Delta^{-1} A A^T \Delta^{-T} P_2, \\
\tilde{\Phi}_{22} &= \Phi_{22} + \lambda^2 P_2 \Delta^{-1} \Delta^{-T} P_2 + P_2 \Delta^{-1} A A^T \Delta^{-T} P_2,
\end{aligned}$$

according to (3.8), $\tilde{\Phi}_{22} < 0$ is a necessary condition for (3.5).

Since (3.5) is not a LMI in a strict sense, it is impossible to directly get the required parameters K_P, K_I and K_D, so it is necessary to convert (3.5) in Theorem 3.1 into a LMI, and we can further obtain the following theorem:

Theorem 3.2. If there exist two matrices P_I and P_D such that

$$sym\left(-BP_I - BP_DB^T\right) + \lambda^2 I + AA^T < 0, \tag{3.9}$$

then P_I and P_D can be obtained by the (3.9), and the PID controller parameter K_I can be obtained by solving

$$K_I = P_I P_2, \tag{3.10}$$

while K_D can be obtained by solving

$$P_I K_D^T = P_D, \tag{3.11}$$

Proof. By pre-multiplying ΔP_2^{-T} and post-multiplying $P_2^{-1}\Delta^T$, $\tilde{\Phi}_{22} < 0$ in Eq (3.8) is equivalent to

$$sym\left(-BK_I P_2^{-1}\Delta^T\right) + \lambda^2 I + AA^T < 0, \tag{3.12}$$

denote P_I and P_D as:

$$P_I = K_I P_2^{-1}, P_D = K_I P_2^{-1} K_D. \tag{3.13}$$

It can be verified that (3.12) holds only when (3.9) holds. Obviously, (3.9) is a LMI related to P_I and P_D, so a set of P_2, K_I matrices can be calculated and Δ can be guaranteed to be invertible. For any $\alpha > 0$, $P_2 = \frac{1}{2}\alpha I$ can be selected.

Next, we will continue to calculate K_P.

Theorem 3.3. If there exist matrices $Q_1 > 0$, Q_P and parameters $\delta > 0$, $\lambda > 0$ such that

$$\Psi = \begin{pmatrix} \psi_{11} & \psi_{12} + \delta^2 I & Q_1 & \Delta^{-1} & \Delta^{-1}A & Q_1 {U_1}^T \\ \psi_{12}^T + \delta^2 I & \psi_{22} & 0 & 0 & 0 & 0 \\ Q_1^T & 0 & -\alpha^{-1} I & 0 & 0 & 0 \\ \Delta^{-T} & 0 & 0 & -\lambda^{-1} I & 0 & 0 \\ A^T\Delta^{-T} & 0 & 0 & 0 & I & 0 \\ U_1 Q_1^T & 0 & 0 & 0 & 0 & I \end{pmatrix} < 0, \tag{3.14}$$

where

$$\begin{aligned} \psi_{11} &= sym\left(\Delta^{-1}AQ_1^T - \Delta^{-1}BQ_P^T\right), \\ \psi_{12} &= -\Delta^{-1}BK_I + \alpha\left(Q_1A^T - Q_PB^T\right)\Delta^{-T}, \\ \psi_{22} &= sym\left(-P_2^T\Delta^{-1}BK_I\right) + \lambda^2 P_2\Delta^{-1}\Delta^{-T}P_2 + P_2\Delta^{-1}AA^T\Delta^{-T}P_2, \end{aligned}$$

with the constraint

$$\frac{\alpha}{2}\lambda_{\max}(Q_1) < \delta, \tag{3.15}$$

then the parameter K_P of PID controller (3.1) can be calculated by $K_P = Q_P^T Q_1^{-T}$.

Proof. Let $Q_1 = P_1^{-1}$, $\Omega_1 = diag\left\{P_1^{-1}, I\right\}$, substitute the obtained P_2, K_I and K_D into (3.8), pre-multiply Ω_1 and post-multiply ${\Omega_1}^T$, we have

$$\begin{pmatrix} \tilde{\psi}_{11} & \tilde{\psi}_{12} \\ \tilde{\psi}_{12}^T & \tilde{\psi}_{22} \end{pmatrix} < 0, \tag{3.16}$$

where

$$\begin{aligned} \tilde{\psi}_{11} &= sym\left(\Delta^{-1}AQ_1^T - \Delta^{-1}BQ_P^T\right) + Q_1\left(P_2 + P_2^T\right)Q_1^T + \lambda^2\Delta^{-1}\Delta^{-T} + \Delta^{-1}AA^T\Delta^{-T} + \tfrac{2}{\lambda^2}Q_1{U_1}^T U_1 {Q_1}^T, \\ \tilde{\psi}_{12} &= -\Delta^{-1}BK_I + \left(Q_1A^T - Q_PB^T\right)\Delta^{-T}P_2 + Q_1P_3 + \lambda^2\Delta^{-1}\Delta^{-T}P_2 + \Delta^{-1}AA^T\Delta^{-T}P_2, \\ \tilde{\psi}_{22} &= sym\left(-P_2^T\Delta^{-1}BK_I\right) + \lambda^2 P_2\Delta^{-1}\Delta^{-T}P_2 + P_2\Delta^{-1}AA^T\Delta^{-T}P_2. \end{aligned}$$

According to the Schur complement lemma [30], (3.16) is equivalent to

$$\Psi = \begin{pmatrix} \psi_{11} & \psi_{12} + Q_1 P_3 & Q_1 & \Delta^{-1} & \Delta^{-1} A & Q_1 {U_1}^T \\ \psi_{12}^T + P_3^T Q_1^T & \psi_{22} & 0 & 0 & 0 & 0 \\ Q_1^T & 0 & -\alpha^{-1} I & 0 & 0 & 0 \\ \Delta^{-T} & 0 & 0 & -\lambda^{-1} I & 0 & 0 \\ A^T \Delta^{-T} & 0 & 0 & 0 & I & 0 \\ U_1 Q_1^T & 0 & 0 & 0 & 0 & I \end{pmatrix} < 0. \tag{3.17}$$

Let $Q_3 = Q_1 P_3 = \delta^2 I$, then when $P_3 = \delta^2 Q_1^{-1}$, Inequality (3.17) is equivalent to Inequality (3.14). According to the Schur complement lemma [30], if inequality

$$P_3 - \frac{1}{4}\alpha^2 P_1^{-1} > 0,$$

or

$$\left(\delta^2 Q_1^{-2} - \frac{1}{4}\alpha^2\right) Q_1 > 0,$$

holds and satisfies (3.15), it can be guaranteed that (3.4) holds.

4. Disturbance observer design

In practical engineering applications, there often exist various disturbances in the system. In this paper, it is assumed that the external interference $d(t)$ is

$$\begin{cases} \dot{\xi}(t) = A_\omega \xi(t) + F g(\xi(t)), \\ d(t) = C_\omega \xi(t), \end{cases} \tag{4.1}$$

where $\xi(t)$ is the state vector of the exogenous system, $\xi(t) \in R^{m\times 1}$; $A_\omega \in R^{m\times m}$, $C_\omega \in R^{m\times m}$, $F \in R^{m\times m}$ are known constant matrices; $g(\xi(t))$ is a known Lipschitz continuous nonlinear function, which satisfies the following assumption:

Assumption 4.1. For any $\xi_1(t)$ and $\xi_2(t)$, the nonlinear function $g(\xi(t))$ satisfies

$$\|g(\xi_1(t)) - g(\xi_2(t))\| \le \left\|\bar{U}(\xi_1(t) - \xi_2(t))\right\|,$$

where $\bar{U}$ is given Lipschitz constant and $\|\cdot\|$ stands for Euclidean norm for vectors.

Compared with those linear external disturbances in [31, 32], the external system in this paper can not only describe linear signals such as constant load, harmonic disturbances, but also nonlinear signals in [33, 34].

For the external disturbance System (4.1), this paper constructs the following disturbance observer:

$$\begin{aligned} &\hat{d}(t) = C_\omega \hat{\xi}(t), \\ &\hat{\xi}(t) = v(t) + Lx(t), \\ &\dot{v}(t) = (A_\omega - LC_\omega)\hat{\xi}(t) - L(Ax(t) + Bu(t) + f(x(t))) + Fg\left(\hat{\xi}(t)\right), \end{aligned} \tag{4.2}$$

where $\hat{\xi}(t)$ is the estimated value of $\xi(t)$, $v(t)$ is the auxiliary vector, and L is the nonlinear gain function of the disturbance observer.

Define the estimation error as $e_\xi(t) = \xi(t) - \hat{\xi}(t)$, then the derivative of $e_\xi(t)$ can be written as

$$\begin{aligned}\dot{e}_\xi(t) &= \dot{\xi}(t) - \dot{\hat{\xi}}(t)\\ &= A_\omega \xi(t) - (A_\omega - LC_\omega)\hat{\xi}(t) - LC_\omega + F\left(g(\xi(t)) - g\left(\hat{\xi}(t)\right)\right)\\ &= (A_\omega - LC_\omega)\left(\xi(t) - \hat{\xi}(t)\right) + F\left(g(\xi(t)) - g\left(\hat{\xi}(t)\right)\right)\\ &= (A_\omega - LC_\omega)e_\xi(t) + F\left(g(\xi(t)) - g\left(\hat{\xi}(t)\right)\right).\end{aligned} \tag{4.3}$$

In the case of nonlinear harmonic disturbances (4.1), if we do nothing, the tracking error $\varepsilon(t)$ will increase sharply compared with the tracking error in (3.2). Next, we will analyze the tracking error $\varepsilon(t)$ and try to minimize it in the upper layer. It is noted that neither the structure nor the parameters of the bottom layer controllers will be changed.

In fact, if we substitute the PID controller (3.1) into (2.5), we will obtain

$$\begin{aligned}\dot{\varepsilon}(t) &= \dot{r}^*(t) - \dot{x}(t)\\ &= \Delta^{-1}\Pi\varepsilon(t) - \Delta^{-1}BK_I s(t)\\ &\quad - \Delta^{-1}\left(BK_P R(t) + BK_I\int_0^t R(t)\,d\tau + BK_D\dot{R}(t)\right)\\ &\quad + \Delta^{-1}\dot{r}^*(t) - \Delta^{-1}C_\omega\xi(t) - \Delta^{-1}Ar^*(t) - \Delta^{-1}f(x(t)),\end{aligned} \tag{4.4}$$

where $R(t) = r(t) - r^*(t)$. Combined with (4.3) and (4.4), the following composite system can be obtained:

$$\begin{cases}\dot{\varepsilon}(t) = \Delta^{-1}\Pi\varepsilon(t) - \Delta^{-1}BK_I s(t) - \Delta^{-1}\left(BK_P R(t) + BK_I\int_0^t R(\tau)\,d\tau + BK_D\dot{R}(t)\right)\\ \qquad + \Delta^{-1}\dot{r}^*(t) - \Delta^{-1}C_\omega\xi(t) - \Delta^{-1}Ar^*(t) - \Delta^{-1}f(x(t)),\\ \dot{s}(t) = \varepsilon(t),\\ \dot{e}_\xi(t) = (A_\omega - LC_\omega)e_\xi(t) + F\left(g(\xi(t)) - g\left(\hat{\xi}(t)\right)\right).\end{cases} \tag{4.5}$$

5. Upper layer dynamic set points adjustment

In Section 4, for those nonlinear harmonic disturbances, we have designed a disturbance observer to estimate them. Next, to ensure the loop outputs $y_i(t)$ can still track the original target r^* under these disturbances, we will try to dynamically adjust the set-points in the upper layer based on the values of the estimated disturbances so that the loop output can still track the original target value under the action of the original controller.

If we adjust the set points as follows:

$$\begin{cases}E\dot{z} = E_1 z + E_2,\\ r(t) = z_2(t) + r^*,\end{cases} \tag{5.1}$$

where

$$E = \begin{bmatrix} I & 0 & 0\\ 0 & I & 0\\ 0 & 0 & 0\end{bmatrix}, E_1 = \begin{bmatrix} 0 & I & 0\\ 0 & 0 & I\\ \Delta^{-1}BK_I & \Delta^{-1}BK_P & \Delta^{-1}BK_D\end{bmatrix}, z(t) = \begin{bmatrix}\int_0^t R(\tau)\,d\tau\\ R(t)\\ \dot{R}(t)\end{bmatrix},$$

$$E_2 = \begin{bmatrix} 0 \\ 0 \\ \Delta^{-1}Ar^* - \Delta^{-1}\dot{r}^*(t) + \Delta^{-1}f(x(t)) + \Delta^{-1}C_\omega\hat{\xi}(t) + K_1\varepsilon(t) + K_2 s(t) \end{bmatrix}.$$

Then we can obtain

$$\begin{aligned} &\Delta^{-1}BK_P R(t) + \Delta^{-1}BK_I\int_0^t R(\tau)\,d\tau + \Delta^{-1}BK_D\dot{R}(t) \\ &= -\Delta^{-1}Ar^* + \Delta^{-1}\dot{r}^*(t) - \Delta^{-1}f(x(t)) - \Delta^{-1}C_\omega\hat{\xi}(t) - K_1\varepsilon(t) - K_2 s(t). \end{aligned} \tag{5.2}$$

Substituting (5.2) into (4.5), the composite system composing of $\varepsilon(t)$, $s(t)$ and $e_\xi(t)$ can be expressed as follows:

$$\begin{aligned} \begin{bmatrix} \dot{\varepsilon}(t) \\ \dot{s}(t) \\ \dot{e}_\xi(t) \end{bmatrix} &= \begin{bmatrix} \Delta^{-1}\Pi + K_1 & K_2 - \Delta^{-1}BK_I & -\Delta^{-1}C_\omega \\ I & 0 & 0 \\ 0 & 0 & A_\omega - LC_\omega \end{bmatrix}\begin{bmatrix} \varepsilon(t) \\ s(t) \\ e_\xi(t) \end{bmatrix} \\ &+ \begin{bmatrix} 0 \\ 0 \\ F \end{bmatrix}\left(g(\xi(t)) - g\left(\hat{\xi}(t)\right)\right). \end{aligned} \tag{5.3}$$

Let $G_{11} = \begin{pmatrix} \Delta^{-1}\Pi & -\Delta^{-1}BK_I \\ I & 0 \end{pmatrix}, G_{22} = \begin{pmatrix} -\Delta^{-1}C_\omega \\ 0 \end{pmatrix}, G_{12} = \begin{pmatrix} I \\ 0 \end{pmatrix}, \bar{F} = \begin{pmatrix} 0 \\ 0 \\ F \end{pmatrix}$, then the composite System (5.3) can be further written as

$$\dot{\bar{x}}(t) = G\bar{x}(t) + \bar{F}\left(g(\xi(t)) - g\left(\hat{\xi}(t)\right)\right),$$

where $\bar{x}(t) = \begin{pmatrix} \varepsilon(t)^T & s(t)^T & e_\xi(t)^T \end{pmatrix}^T, G = \begin{pmatrix} G_{11} + G_{12}\bar{K} & G_{22} \\ 0 & A_\omega - LC_\omega \end{pmatrix}, \bar{K} = \begin{bmatrix} K_1 & K_2 \end{bmatrix}$.

Theorem 5.1. For a given $\tau > 0$, if there exist $\Gamma_1 \in R^{m\times m}$, $X \in R^{l\times m}$ and $Y \in R^{m\times m}$ such that the following LMI holds:

$$\begin{pmatrix} \Xi_1 & \Xi_2 & 0 & 0 \\ * & \Xi_3 & F & \bar{U}^T \\ * & * & -\tau I & 0 \\ * & * & * & -\tau^{-1}I \end{pmatrix} < 0, \tag{5.4}$$

where

$$\begin{aligned} \Xi_1 &= sym(G_{11}\Gamma_1 + G_{12}X), \\ \Xi_2 &= G_{22}, \\ \Xi_3 &= sym(A_\omega - YC_\omega), \end{aligned}$$

then the gains K_1, K_2 in (5.1) and the disturbance observer gain L in (4.2) can be obtained by:

$$\begin{aligned} \begin{bmatrix} K_1 & K_2 \end{bmatrix} &= X\Gamma_1^{-1} \\ L &= Y, \end{aligned} \tag{5.5}$$

and the composite System (4.5) is exponentially stable.

Proof. In order to prove the stability of the error composite System (5.3), we construct the following Lyapunov function: $V_2 = \bar{x}^T(t)\bar{P}\bar{x}(t)$ where $\bar{P}=\begin{bmatrix} \bar{P}_1 & 0 \\ 0 & I \end{bmatrix} > 0$. Taking the derivative of $V_2(t)$ with respect to t yields

$$\begin{aligned}
\dot{V}_2 &= 2\bar{x}^T\bar{P}\dot{\bar{x}} \\
&= 2\bar{x}^T\bar{P}\left(G\bar{x} + \bar{F}\left(g(\xi(t)) - g\left(\hat{\xi}(t)\right)\right)\right) \\
&= 2\bar{x}^T\bar{P}G\bar{x} + 2\bar{x}^T\bar{P}\bar{F}\left(g(\xi(t)) - g\left(\hat{\xi}(t)\right)\right) \\
&= W(t)^T\Lambda_1 W(t) + \tau\left\|g(\xi(t)) - g\left(\hat{\xi}(t)\right)\right\|^2,
\end{aligned}$$

where $W(t) = \begin{pmatrix} \bar{x}(t) \\ g(\xi(t)) - g\left(\hat{\xi}(t)\right) \end{pmatrix}$, $\Lambda_1 = \begin{pmatrix} sym\left(\bar{P}G\right) & \bar{P}^T\bar{F} \\ * & -\tau I \end{pmatrix}$.

According to Assumption 4.1,

$$\left\|g(\xi(t)) - g\left(\hat{\xi}(t)\right)\right\| \le \left\|\bar{U}\left(\xi(t) - \hat{\xi}(t)\right)\right\| = \left\|\bar{U}e_{\xi}(t)\right\| \le \left\|\bar{U}H\bar{x}(t)\right\|,$$

then $\dot{V}_2 \le W^T(t)\Lambda_2 W(t)$ where $\Lambda_2 = \begin{pmatrix} sym\left(\bar{P}G\right) + \tau H^T\bar{U}^T\bar{U}H & \bar{P}^T\bar{F} \\ * & -\tau I \end{pmatrix}$, $H = \begin{pmatrix} 0 & 0 & I \end{pmatrix}$.

Let $\bar{P}_1 = \Gamma_1^{-1}$. By using (5.5) and then pre- and post-multiplying (5.4) with diag $\left\{\bar{P}_1, I, I, I\right\}$, we have

$$\begin{pmatrix} \Psi_1 & \Psi_2 & 0 & 0 \\ * & \Psi_3 & F & \bar{U}^T \\ * & * & -\tau I & 0 \\ * & * & * & -\tau^{-1}I \end{pmatrix} < 0, \tag{5.6}$$

where

$$\begin{aligned}
\Psi_1 &= sym\left[\bar{P}_1\left(G_{11} + G_{12}\bar{K}\right)\right], \\
\Psi_2 &= \bar{P}_1 G_{22}, \\
\Psi_3 &= sym\left(A_\omega - LC_\omega\right).
\end{aligned}$$

Substitute $\dot{\bar{x}}(t) = G\bar{x}(t) + \bar{F}\left(g(\xi(t)) - g\left(\hat{\xi}(t)\right)\right)$ into (5.6), we get

$$\begin{pmatrix} sym\left(\bar{P}G\right) & \bar{P}^T\bar{F} & H^T\bar{U}^T \\ \bar{F}^T\bar{P} & -\tau I & 0 \\ \bar{U}H & 0 & -\tau^{-1}I \end{pmatrix} < 0.$$

According to the Schur complement lemma [30], it is easy to obtain

$$\Lambda_2 < 0,$$

denote $\chi_1 \triangleq |\lambda_{\max}(\Lambda_2)| > 0$, $\chi_2 \triangleq \lambda_{\max}\left(\bar{P}\right)$ and get $\Lambda_2 \le -\chi_1 I$, then

$$\dot{V}_2 \le W(t)^T\Lambda_2 W(t) \le -\chi_1\|\bar{x}(t)\|^2 \le -\chi_1\chi_2^{-1}V, \tag{5.7}$$

from (5.7), we get

$$V_2(\bar{x}(t)) \le V_2(\bar{x}(0))\, e^{-\chi_1\chi_2^{-1}t},$$

which means that System (5.3) is exponentially stable, i.e., the composite System (4.5) is exponentially stable in the presence of disturbances (4.1).

In summary, the algorithm in this paper can be listed as follows:

Step 1. Solve the LMI in (3.9) to get P_I and P_D;

Step 2. Let $P_2 = (1/2)\,\alpha I$, get K_I by $K_I = P_I P_2$, and get K_D through $P_I K_D^T = P_D$;

Step 3. Solve LMIs (3.14) and (3.15) to obtain Q_1 and Q_P;

Step 4. Obtain K_P from $K_P = Q_P^T Q_1^{-T}$ and construct controller (3.1);

Step 5. Solve Eq (5.4) to obtain X, Γ_1 and Y, and get L and $\bar{K}$ from $L = Y$ and $\bar{K} = X\Gamma_1^{-1}$. Construct a disturbance observer (4.2) and adjust the set point value according to (5.1).

6. Simulations

Most zinc smelting enterprises use goethite method to precipitate iron from zinc sulfate solution. After the introduced indium post deposition liquid is passed into the reactor for chemical reaction, the post deposition liquid with ferrous iron will be obtained. The goethite method for ion concentration control is shown in Figure 2. In [14], the process of iron deposition consists of four ferric precipitation reactors. Different concentrations of oxygen need to be fed to each branch tube because the low ferric ion concentration declines during the reaction. However, those small part of oxygen retention existing in the pipe reacting with heat might affect the actual oxygen concentration. In addition, the air pressure and temperature of the intake pipe generate periodic fluctuations, and mutual friction and thermal fluctuation are also generated between the components of the pipe. According to the three chemical reaction processes in the iron precipitation process of goethite method, the concentration of oxygen which is fed into each pipe can be regarded as the system state, the input current as the control input, the concentration of ferrous iron after the reaction as the system output, and the factors such as thermal fluctuation, mutual friction between pipeline components and periodic fluctuation of air pressure and temperature can be regarded as uncertain perturbation. Then the chemical reaction rate of ferrous iron can be obtained in combination with the chemical reaction kinetics, the corresponding mass balance equation can be established through the principle of material conservation, and the mechanism model of the reactor in the iron precipitation process can be finally determined as [35]:

$$\begin{cases} \dot{x}(t) = Ax(t) + Bu(t) + f(x(t), t) + d(t), \\ y(t) = Cx(t), \end{cases}$$

where $A = \begin{bmatrix} -1 & 1 & 0 & 0 \\ 1 & 1 & 0 & 0 \\ 0 & 0 & 1 & -1 \\ 0 & 0 & -2 & -1 \end{bmatrix}$, $B = \begin{bmatrix} 1 & 0 & 0 & 0 \\ 0 & 1 & 0 & 0 \\ 0 & 0 & 1 & 0 \\ 0 & 0 & 0 & 1 \end{bmatrix}$, $f = \begin{bmatrix} -0.3\sin(x_1) \\ 0 \\ 0.3\cos(x_3) \\ 0 \end{bmatrix}$, $d(t) = \begin{bmatrix} d_1 \\ d_2 \\ d_3 \\ d_4 \end{bmatrix}$; x is the oxygen concentration of each branch pipe; u is the control input current under the action of external disturbance $d(t)$; f is the concentration of residual oxygen in the pipeline after chemical reaction, system output y is the concentration of ferrous iron after the reaction.

The schematic diagram of ion concentration control for goethite process can be illustrated as follows:

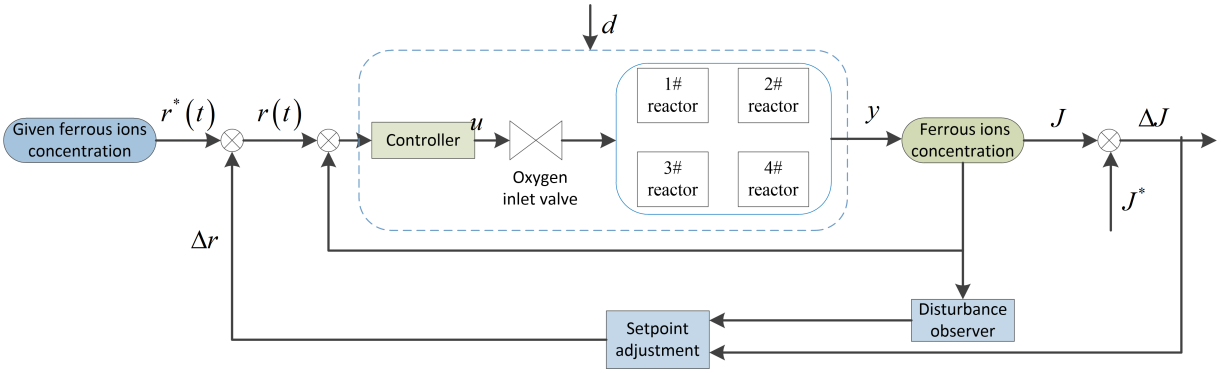

Figure 2. Schematic diagram of ion concentration control of goethite process.

The initial state of the state vector is set to be $\begin{bmatrix} x_1(0) & x_2(0) & x_3(0) & x_4(0) \end{bmatrix} = \begin{bmatrix} 0 & 0 & 0 & 0 \end{bmatrix}$. Also we set the target value as $\begin{bmatrix} r_1^*(t) & r_2^*(t) & r_3^*(t) & r_4^*(t) \end{bmatrix} = \begin{bmatrix} 107.4 & 53.7 & 17.9 & 3.6 \end{bmatrix}$ [14].

Define the system performance index as

$$J=(y_1(t)-r_1^*(t))^2+(y_2(t)-r_2^*(t))^2+(y_3(t)-r_3^*(t))^2+(y_4(t)-r_4^*(t))^2,$$

where $r^*(t)$ is the set target value, $y(t)$ is the system output ion concentration, and J is the sum of squares of tracking error.

According to Theorems 3.2 and 3.3, the controller parameters can be obtained by

$$K_I = \begin{bmatrix} 1.0105 & 0 & 0 & 0 \\ 0 & 1.0105 & 0 & 0 \\ 0 & 0 & 1.0105 & 0 \\ 0 & 0 & 0 & 1.0105 \end{bmatrix}, \quad K_D = \begin{bmatrix} 1 & 0 & 0 & 0 \\ 0 & 1 & 0 & 0 \\ 0 & 0 & 1 & 0 \\ 0 & 0 & 0 & 1 \end{bmatrix},$$

$$K_P = \begin{bmatrix} 7.7968 & 0.9893 & 0 & 0 \\ 1.0106 & 7.9729 & 0 & 0 \\ 0 & 0 & 8.8254 & -1.9984 \\ 0 & 0 & -3.5634 & 17.0733 \end{bmatrix}.$$

For the harmonic disturbances $d(t)$ as in (4.1), the parameters are selected as

$$A_\omega = \begin{pmatrix} 0 & 6 & 0 & 0 \\ -6 & 0 & 0 & 0 \\ 0 & 0 & 0 & 6 \\ 0 & 0 & -6 & 0 \end{pmatrix}, C_\omega = \begin{pmatrix} 0.1 & 0 & 0 & 0 \\ 0 & 0.1 & 0 & 0 \\ 0 & 0 & 0.1 & 0 \\ 0 & 0 & 0 & 0.1 \end{pmatrix}, F = \begin{pmatrix} 1 & 0 & 0 & 0 \\ 0 & 1 & 0 & 0 \\ 0 & 0 & 1 & 0 \\ 0 & 0 & 0 & 1 \end{pmatrix}, g = \begin{bmatrix} 0.5\sin(\xi_1) \\ -0.5\cos(\xi_2) \\ 0.5\sin(\xi_3) \\ -0.5\cos(\xi_4) \end{bmatrix}.$$

In the presence of exogenous disturbances, the comparison results of the system output ion concentration, the error between the tracking target and the actual ion concentration and the system performance indices are shown in Figures 3–5, respectively.

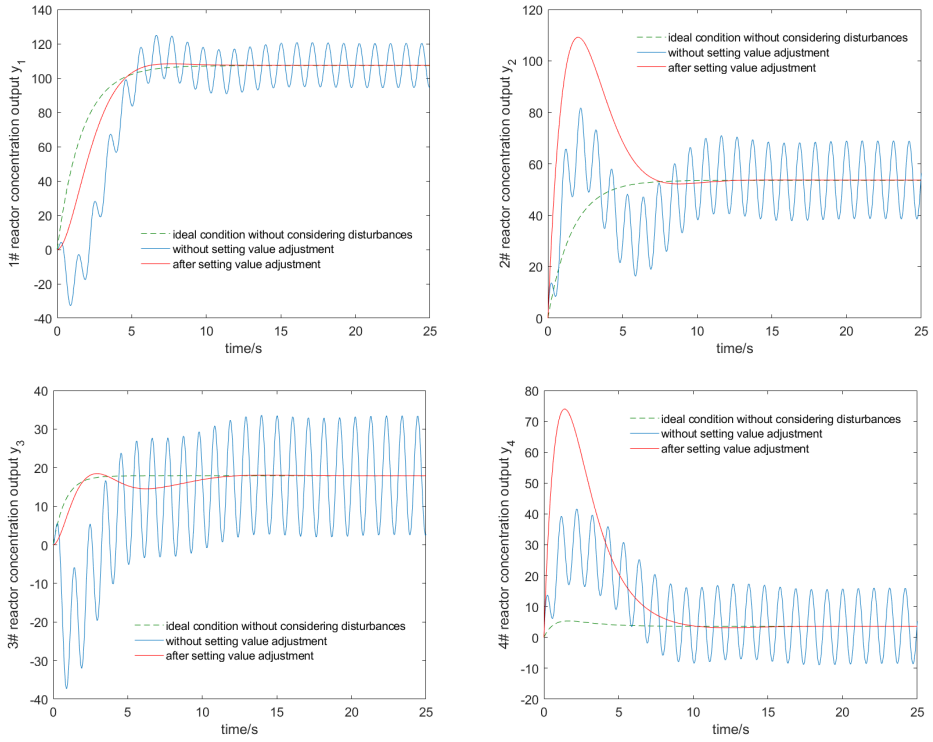

Figure 3. Comparison of ion concentration output.

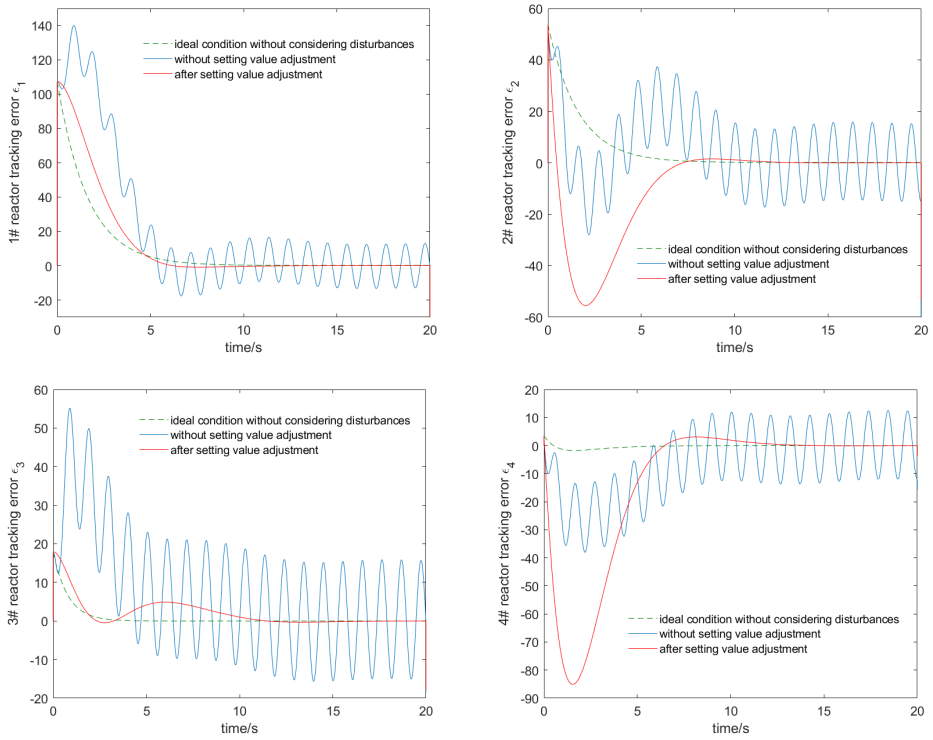

Figure 4. Comparison of tracking error.

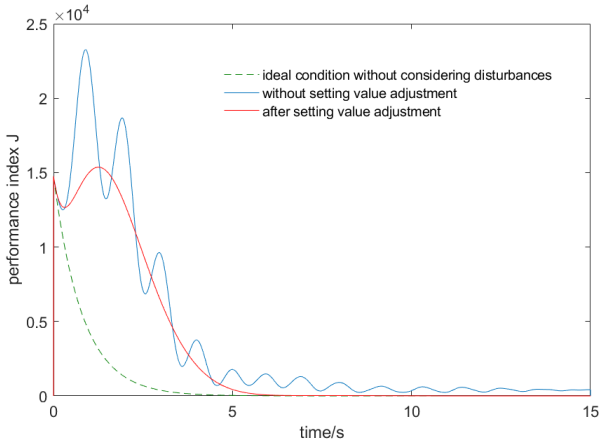

Figure 5. Comparison of the performance indexes.

In the ideal conditions, the tracking error ε finally tends to zero. However, when there exist exogenous disturbances (4.1) in the system, if the set value is not adjusted, the ion concentration y output from the four reactors will fluctuate near the ideal value. As shown by the blue line in Figure 3, the fluctuation ranges of the four reactors are as follows: $-12.9 \sim 12.9\,(mmol/L)$, $-15.0 \sim 15.0\,(mmol/L)$, $-15.05 \sim 15.05\,(mmol/L)$, $-11.95 \sim 11.95\,(mmol/L)$. At the same time, the system tracking error ε of the four reactors fluctuates near zero. As shown by the blue line in Figure 4, the fluctuation ranges of tracking error ε are as follows: $-12.8 \sim 12.8\,(mmol/L)$, $-15.1 \sim 15.1\,(mmol/L)$, $-15.7 \sim 15.7\,(mmol/L)$, $-11.38 \sim 11.38\,(mmol/L)$. The blue line in Figure 5 is the performance index J of the system in the presence of exogenous disturbances (4.1). When there exist exogenous disturbances and the set value is not adjusted, the curve fluctuates frequently up and down.

It can be seen that in the presence of exogenous disturbances (4.1), if the controller is not changed and no adjustment is made in the upper layer, the system performance will deteriorate seriously.

According to Theorem 5.1, we can get

$$L=\begin{bmatrix} 15.1182 & 0 & 0 & 0 \\ 0 & 15.1182 & 0 & 0 \\ 0 & 0 & 15.1182 & 0 \\ 0 & 0 & 0 & 15.1182 \end{bmatrix},$$

$$K_1=\begin{bmatrix} -1.238\times10^3 & 0.178\times10^3 & 0 & 0 \\ 0.178\times10^3 & -1.238\times10^3 & 0 & 0 \\ 0 & 0 & -3.182\times10^3 & 0.128\times10^3 \\ 0 & 0 & -0.405\times10^3 & -7.316\times10^3 \end{bmatrix},$$

$$K_2=\begin{bmatrix} -3.201\times10^5 & 1.077\times10^3 & 0 & 0 \\ 1.077\times10^3 & -3.201\times10^5 & 0 & 0 \\ 0 & 0 & -9.679\times10^5 & 0.679\times10^3 \\ 0 & 0 & 0.679\times10^3 & -9.679\times10^5 \end{bmatrix}.$$

Figure 6 is the set point value adjustment. After the set value is readjusted, the ion concentration output y of the system quickly reaches the set point. At the same time, the tracking error ε of the system

can not only tend to zero, but also respond quickly. The performance index J of the system gradually improves and the system reaches a stable state, as shown by the red line in Figures 3–5.

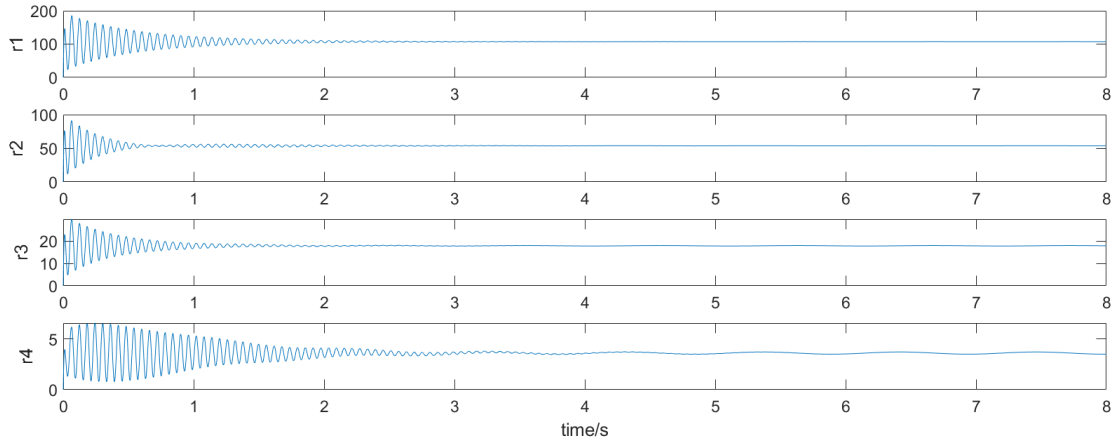

Figure 6. Setpoint adjustment process.

7. Conclusions

This paper mainly studies a two-level optimal setting control for nonlinear systems with exogenous disturbances. In order to make the disturbance model more suitable for engineering practice, the additional disturbances caused by external system nonlinearity is considered. Firstly, the PID controller is used in the bottom loop, and the PID controller parameters are obtained according to the Lyapunov theory and the LMI method. Secondly, for nonlinear harmonic disturbances, a disturbance observer is designed in the upper layer to estimate these nonlinear disturbances. Finally, the set point value is dynamically adjusted to minimize the impact caused by disturbances or noises. This method can track the target value well without changing the structure or parameters of those bottom layer controllers of the whole system.

8. Future work

In this paper, we only consider nonlinear loop systems satisfying Lipschitz conditions, and the external disturbances are of harmonic type. In fact, the system might be complex, there probably exist composite disturbances, and the practical systems will generally have requirements on inputs and outputs. So, we believe the work includes data-based modeling, multi-objectives, composite disturbances or input/output constraints will be quite promising.

Acknowledgments

The work reported was jointly supported by the National Natural Science Foundation of China under grants 61573190, 61973168 and Project 333 of Jiangsu Province under Grant BRA2020067.

Conflict of interest

The authors declare that there is no conflict of interests.

References

1. A. Wang, P. Zhou, H. Wang, Performance analysis for operational optimal control for complex industrial processes under small loop control errors, In: *Proceedings of the 2014 international conference on advanced mechatronic systems*, 2014. http://doi.org/10.1109/ICAMechS.2014.6911643
2. T. Chai, S. J. Qin, H. Wang, Optimal operational control for complex industrial processes, *Annu. Rev. Control*, **38** (2014), 81–92. http://doi.org/10.1016/j.arcontrol.2014.03.005
3. L. Yin, H. Wang, X. Yan, H. Zhang, Disturbance observer-based dynamic optimal setting control, *IET Control Theory A.*, **12** (2018), 2423–1432. http://doi.org/10.1049/iet-cta.2018.5013
4. L. Yin, H. Wang, L. Guo, H. Zhang, Data-driven pareto-de-based intelligent optimal operational control for stochastic processes, *IEEE T. Syst. Man Cy. Syst.*, **51** (2021), 4443–4452. http://doi.org/10.1109/TSMC.2019.2936452
5. W. Dai, G. Huang, F. Chu, T. Chai, Configurable platform for optimal-setting control of grinding processes, *IEEE Access*, **5** (2017), 26722–26733. http://doi.org/10.1109/ACCESS.2017.2774001
6. M. Li, P. Zhou, H. Wang, T. Chai, Nonlinear multiobjective mpc-based optimal operation of a high consistency refining system in papermaking, *IEEE T. Syst. Man Cy. Syst.*, **50** (2017), 1208–1215. http://doi.org/10.1109/TSMC.2017.2748722
7. P. Zhou, T. Chai, H. Wang, Intelligent optimal-setting control for grinding circuits of mineral processing process, *IEEE T. Autom. Sci. Eng.*, **6** (2009), 730–743. http://doi.org/10.1109/TASE.2008.2011562
8. Y. Jiang, J. Fan, T. Chai, J. Li, F. L. Lewis, Data-driven flotation industrial process operational optimal control based on reinforcement learning, *IEEE T. Ind. Inform.*, **14** (2018), 1974–1989. http://doi.org/10.1109/TII.2017.2761852
9. Y. Zhou, Q. Zhang, H. Wang, P. Zhou, T. Chai, Ekf-based enhanced performance controller design for nonlinear stochastic systems, *IEEE T. Automat. Contr.*, **63** (2018), 1155–1162. http://doi.org/10.1109/TAC.2017.2742661
10. L. Dong, X. Wei, H. Zhang, Anti-disturbance control based on nonlinear disturbance observer for a class of stochastic systems, *T. I. Meas. Control*, **41** (2019), 1665–1675. http://doi.org/10.1177/0142331218787608
11. S. Xie, Y. Xie, F. Li, C. Yang, W. Gui, Optimal setting and control for iron removal process based on adaptive neural network soft-sensor, *IEEE T. Syst. Man Cy. Syst.*, **50** (2020), 2408–2420. http://doi.org/10.1109/TSMC.2018.2815580
12. L. Guo, H. Wang, *Stochastic distribution control system design: A convex optimization approach*, London: Springer, 2010. http://doi.org/10.1007/978-1-84996-030-4

13. Y. Liu, K. Fan, Q. Ouyang, Intelligent traction control method based on model predictive fuzzy pid control and online optimization for permanent magnetic maglev trains, *IEEE Access*, **9** (2021), 29032–29046. http://doi.org/10.1109/ACCESS.2021.3059443

14. X. Zhou, J. Zhou, C. Yang, W. Gui, Set-point tracking and multi-objective optimization-based pid control for the goethite process, *IEEE access*, **6** (2018), 36683–36698. http://doi.org/10.1109/ACCESS.2018.2847641

15. C. Liu, Z. Gong, K. L. Teo, J. Sun, L. Caccetta, Robust multi-objective optimal switching control arising in 1,3-propanediol microbial fed-batch process, *Nonlinear Anal. Hybri.*, **25** (2017), 1–20. http://doi.org/10.1016/j.nahs.2017.01.006

16. C. Liu, Z. Gong, H. W. J. Lee, K. L. Teo, Robust bi-objective optimal control of 1,3-propanediol microbial batch production process, *J. Process Contr.*, **78** (2019), 170–182. http://doi.org/10.1016/j.jprocont.2018.10.001

17. B. Li, Y. Wang, K. Zhang, G. R. Duan, Constrained feedback control for spacecraft reorientation with an optimal gain, *IEEE T. Aero. Elec. Sys.*, **57** (2021), 3916–3926. http://doi.org/10.1109/TAES.2021.3082696

18. J. F. Qiao, Y. Hou, H. G. Han, Optimal control for wastewater treatment process based on an adaptive multi-objective differential evolution algorithm, *Neural Comput. Applic.*, **31** (2019), 2537–2550. http://doi.org/10.1007/s00521-017-3212-4

19. A. Yan, T. Chai, W. Yu, Z. Xu, Multi-objective evaluation-based hybrid intelligent control optimization for shaft furnace roasting process, *Control Eng. Pract.*, **20** (2012), 857–868. http://doi.org/10.1016/j.conengprac.2012.05.001

20. Z. Civelek, E. Cam, M. Luy, H. Mamur, Proportional-integral-derivative parameter optimisation of blade pitch controller in wind turbines by a new intelligent genetic algorithm, *IET Renew. Power Gen.*, **10** (2016), 1220–1228. http://doi.org/10.1049/iet-rpg.2016.0029

21. X. Cong, L. Guo, PID control for a class of nonlinear uncertain stochastic systems, In: *2017 IEEE 56th annual conference on decision and control (CDC)*, 2017. http://doi.org/10.1109/CDC.2017.8263728

22. K. Guo, J. Jia, X. Yu, L. Guo, Dual-disturbance observers-based control of uav subject to internal and external disturbances, In: *2019 Chinese automation congress (CAC)*, 2019. http://doi.org/10.1109/CAC48633.2019.8997330

23. C. Zhao, L. Guo, Control of nonlinear uncertain systems by extended pid, *IEEE T. Automat. Contr.*, **66** (2021), 3840–3847. http://doi.org/10.1109/TAC.2020.3030876

24. C. Zhao, L. Guo, PID control for a class of non-affine uncertain systems, In: *2018 37th Chinese control conference (CCC)*, 2018. http://doi.org/10.23919/ChiCC.2018.8483587

25. S. Yuan, C. Zhao, L. Guo, Decentralized PID control of multi-agent systems with nonlinear uncertain dynamics, In: *2017 36th Chinese control conference (CCC)*, 2017. http://doi.org/10.23919/ChiCC.2017.8028765

26. P. Thampi, G. Raghavendra, Intelligent model for automating PID controller tuning for industrial water level control system, In: *2021 International conference on design innovations for 3Cs compute communicate control (ICDI3C)*, 2021. http://doi.org/10.1109/ICDI3C53598.2021.00039
27. H. Tsukamoto, S. J. Chung, Robust controller design for stochastic nonlinear systems via convex optimization, *IEEE T. Automat. Contr.*, **66** (2021), 4731–4746. http://doi.org/10.1109/TAC.2020.3038402
28. L. Guo, H. Wang, PID controller design for output pdfs of stochastic systems using linear matrix inequalities, *IEEE T. Syst. Man Cy. B*, **35** (2005), 65–71. http://doi.org/10.1109/TSMCB.2004.839906
29. C. Zhao, L. Guo, PID controller design for second order nonlinear uncertain systems, *Sci. China Inf. Sci.*, **60** (2017), 022201. http://doi.org/10.1007/s11432-016-0879-3
30. P. Gahinet, A. Nemirovskii, A. J. Laub, M. Chilali, The LMI control toolbox, In: *Proceedings of 1994 33rd IEEE conference on decision and control*, 1994. http://doi.org/10.1109/CDC.1994.411440
31. X. Wei, L. Dong, H. Zhang, X. Hu, J. Han, Adaptive disturbance observer-based control for stochastic systems with multiple heterogeneous disturbances, *Int. J. Robust Nonlin.*, **29** (2019), 5533–5549. http://doi.org/10.1002/rnc.4683
32. X. Wei, S. Sun, Elegant anti-disturbance control for discrete-time stochastic systems with nonlinearity and multiple disturbances, *Int. J. Control*, **91** (2018), 706–714. http://doi.org/10.1080/00207179.2017.1291996
33. Z. Ding, Output regulation of uncertain nonlinear systems with nonlinear exosystems, *IEEE T. Automat. Contr.*, **51** (2006), 498–503. http://doi.org/10.1109/TAC.2005.864199
34. M. Lu, J. Huang, A class of nonlinear internal models for global robust output regulation problem, *Int. J. Robust Nonlin.*, **25** (2015), 1831–1843. http://doi.org/10.1002/rnc.3180
35. Y. Xie, S. Xie, Y. Li, C. Yang, W. Gui, Dynamic modeling and optimal control of goethite process based on the rate-controlling step, *Control Eng. Pract.*, **58** (2017), 54–65. http://doi.org/10.1016/j.conengprac.2016.10.001

AIMS Press